Accelerated Fluorine-19 MRI Using Compressed Sensing

Lawrence Lechuga

Abstract— In recent years, Fluorine-19 MRI has grown in interest due to its ability to be applied to cell tracking and immunotherapy based imaging. A class of F-19 contrast agents known as Perfluorocarbons (PFC) have shown promise as a cell-labeling agent due to its chemical and physiologic inert nature, and the relatively strong signal of these structures. However, F-19 MRI is plagued by low SNR, which results in long scan times. In an attempt to increase the SNR efficiency, Compressed Sensing (CS) was explored as a method to accelerate the acquisition process. In this experiment, a phantom was loaded with 4 vials of known concentration perfluoropolyether (PFPE) and a 2D Fast Spin Echo (FSE) was used to acquire a fully sampled dataset. The data was then retroactively undersampled at various Acceleration Factors (AF) and reconstructed using an L1-Norm in the image domain. These theoretical accelerated images' SNR and Structural Similarity Index (SSIM) were compared with the fully sampled data set in order to evaluate performance. Results show a modest SSIM was achieved with AF ≤ 4, while showing an unexpected boost in the apparent SNR. In this experiment, it was demonstrated that CS is a promising method to improve the SNR efficiency for F-19 MRI, while preserving imaging integrity.

I. Introduction

Much progress has been made in the area of immunotherapy and cellular therapy in recent years. However, one limiting factor in increasing efficacy is the lack of knowledge in trafficking dynamics. Currently, methods for studying the dynamics *in-vivo* rely on imaging labeled cells. Many methods incubate cells with nanoparticles (iron or gadolinium) to induce uptake. Subsequent MRI will produce images with susceptibility induced signal drop out in regions of nanoparticle presence. While it can be very sensitive, signal-void detection produces magnetic field distortions which makes cellular quantification difficult.

More recently, Fluorine-19 MRI has had increase in use for cell tracking and quantification for various immunotherapies and cell-trafficking studies. ^{19}F MRI provides many benefits over the more common iron nanoparticle ^{1}H MRI. ^{19}F labeled cells produce positive signal and have a negligible endogenous background signal, which makes it ideal for targeted imaging and spin quantification.

Exogenous ^{19}F can be introduced via nanoemulsions of perfluorocarbons (PFCs). Two PFCs of interest are perfluoropolyether (PFPE) and perfluoro-15-crown-5-ether (PFCE). These agents have many beneficial properties such as simple resonant peaks, chemically and biologically inert, and ideal size for phagocytosis in many cell types. Previous studies have validated ^{19}F MRI in preclinical studies tracking various cell types.

While F-19 has these many strong features in regard to cell tracking, it also has many hurdles to overcome before it can be more practical. Due to the relatively low signal compared to that of Proton MRI, the SNR is typically very low in these in-vivo scans. This is typically rectified by performing many averages in order to boost signal; however, this is not practical in the realm of clinical imaging as time constraints will be the limiting factor for overall SNR. Given that the F-19 signal is targeted to specific location, it is very sparse in the pixel representation, which makes it a natural candidate for compressed sensing applications. This method of undersampling and reconstruction can possibly provide a viable route to accelerate imaging and increase the SNR efficiency (SNR/t).

The purpose of this experiment is to theoretically show that pseudo-randomly undersampled Fluorine-19 images can be reconstructed with minimal losses to image integrity while accelerating acquisition by a factor of 2-8. This will be accomplished by retroactively undersampling a fully sampled data set and using some image and compression quality metrics to evaluate the CS reconstructed images to the reference data set.

II. Methods and Materials

A. Data Acquisition

All data was acquired with a 4.7 T Varian horizontal bore small animal scanner. A cylindrical phantom was loaded with 4 vials of PFPE with known concentrations and a blank water vial in a clockwise order of decreasing concentration of PFPE. An axial representation of this set up and the inserts can be seen in Figure 1.
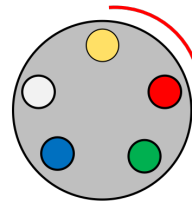
Figure 1: Axial representation of the phantom and PFPE inserts. Inserts were placed in order of decreasing concentration in a clockwise direction.

The fully sampled data set, or reference image data was acquired in 25 minutes with a 2D Multislice Fast Spin Echo (FSE) with an Echo Train Length (ETL) of 8.

B. Undersampling

To acquire the theoretically undersampled data sets, the reference image k-space was retroactively undersampled by 50%, 25%, and 12.5%, for theoretical Acceleration Factors (AF) of 2, 4, and 8. This was accomplished with the use of the SparseMRI toolkit by using a 1D Monte-Carlo based PDF to generate a logical 2D mask that represents the phase encoding steps to acquire and the steps to skip and zero fill [1]. The PDF generated masks, shown in Figure 2, emphasize denser sampling in the center of k-space, with less emphasis as the distance from the origin increases.

The undersampling masks there then multiplied with the reference data set to produce 3 undersampled data sets at a theoretical AF of 2, 4, and 8.

C. Reconstruction

To reconstruct the theoretic CS data sets, a toolkit known as BART was used (Berkeley Advanced Reconstruction Toolkit) was used [1]. This toolkit has a vast array of functions and tools that can streamline the reconstructions and sparsity transforms to a single line of code.

Given that the images are sparse in the image domain, no transform was needed for the reconstruction. The reconstructions were performed using a least squares reconstruction with an L1-norm regularization as seen in (1).

$$\text{argmin}[\ \frac{1}{2}\|F_u\ \hat{x} - y\|^2 + \lambda\|\hat{x}\|_1\ ] \tag{1}$$

Where x is the estimated signal, $F_u x$ is the undersampled fourier transform of the estimate, y are the samples of the fourier transform that were acquired, and λ is the regularization parameter. However, upon reconstruction it was apparent that the fidelity of the resultant image is highly sensitive to the choice of the regularization parameter. To arrive at an optimized regularization, multiple reconstructions were performed over a range of regularization parameters in order to assess the parameter that generated the highest quality image.
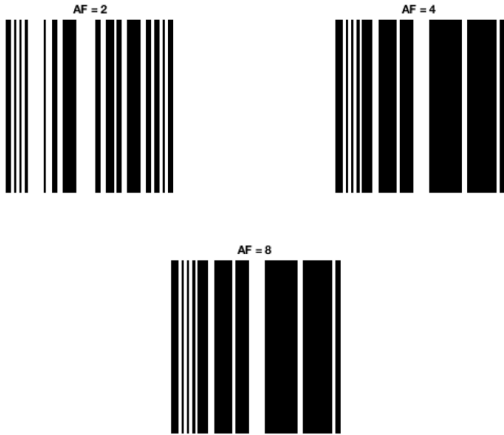
D. Imaging Quality Metrics

To assess the image quality, the SNR and SSIM were evaluated for each reconstruction at the various respective regularizations. The SSIM is a metric originally developed to assess the quality of a compressed image relative to a reference. This metric is not measured in absolute error like MSE or PSNR, but with a perception-based model that attempts to take human perception of structural similarity into account [2].

The SSIM takes into account structural changes in the image, but in order to evaluate the changes in signal strength within regions of interest, an SNR estimate was implemented on the optimal regularized CS images in two ways. The first was to take a noise measurement far from the F-19 signal and use its standard deviation to represent the noise in the image. The images were then scaled by this noise estimate in order to place them into arbitrary units of SNR. Second, a noise measurement was taken from the raw CS reconstructed images at the optimal regularization. Then, ROIs were drawn around the vials of interest, with special care to not include the border of the vials. The mean value of each ROI was then divided by the noise to provide an SNR estimate of each vial in each of the reconstructions. This allows for an objective view of how the signal is changing in each of the vials of interest.

It is important to note that the SNR measures mentioned above are not entirely accurate due to the non-linear nature of the reconstruction. This can create a non-bivariate gaussian noise distribution that will alter the accuracy of the comparison across the data sets. However, the literature suggests that the effect on accuracy will be minimal given that the AF are small [3,4].

III. RESULTS

A. Structural Similarity

The reconstructions were performed at various regularization parameters and plotted against their respective SSIM, which can be seen in Figure 3.

Figure 2: Undersampling masks generated with SparseMRI 1D PDF generator. AF = 2 (left), AF = 4 right), and AF =8 (bottom).
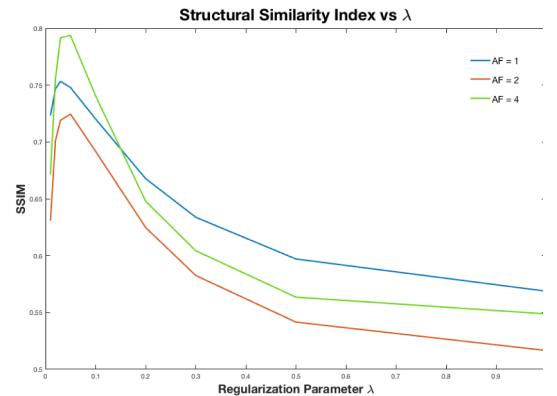

Figure 3: The structural similarity index across the regularization parameters for 0.01 to 1.0 for each AF.

These results showed that the optimal λ for AF of 2, 4, 8 occurred at 0.02, 0.03, 0.05, respectively. For the remainder of the discussion, only the optimal reconstructions will be considered.

B. SNR Estimation

The first SNR estimate can be seen in Figure 4, which shows an increase in visibility of the left-most vial, but also shows an amplification of artifacts. It is important to note that the artifacts present in the CS images are also present in the reference data set but are merely amplified in appearance. The artifacts being: FSE blurring due to large ETL values and chemical shift artifacts due to PFPE's multiple resonance peaks.

The second SNR estimate using the ROI-based evaluation showed similar results to the first method. Each ROI showed increased SNR as the acceleration factor was increased (see Figure 5). This could be due to the increased denoising that occurs at the increased acceleration factors. This reasoning was validated by the overall decrease in the standard deviation of the noise measurement as AF was increased.

IV. CONCLUSION

The acceleration factors of 2, 4, and 8 all show strong structural integrity, increased detectability of the low signal regions, and an increase in the artifact intensity. This method demonstrates that compressed sensing is a viable route to explore in order to increase the SNR efficiency. However, the increase in visibility in all the regions of interest as AF increased was somewhat unexpected. This apparent issue can be addressed in further work. Some additional areas for future work include using contrast agents with a single resonant peak (PFCE) and reconstructions using alternate sparsity transforms, like Total Variation.

Figure 4: SNR measurements at each of the ROIs. Note the increase in SNR from the reference data set (blue) to the AF = 2 (orange) and AF = 4 (yellow).

REFERENCES

[1] BART. http://people.eecs.berkeley.edu/~mlustig/Software.html
[2] Wang, Zhou, Eero P. Simoncelli, and Alan C. Bovik. "Multiscale structural similarity for image quality assessment." The Thrity-Seventh Asilomar Conference on Signals, Systems & Computers, 2003. Vol. 2. Ieee, 2003.
[3] Zhong, Jia, et al. "Accelerated fluorine-19 MRI cell tracking using compressed sensing." Magnetic resonance in medicine 69.6 (2013): 1683-1690.
[4] Liang, Sayuan, et al. "Comparison of different compressed sensing algorithms for low SNR 19F MRI applications—Imaging of transplanted pancreatic islets and cells labeled with perfluorocarbons." NMR in Biomedicine 30.11 (2017): e3776.
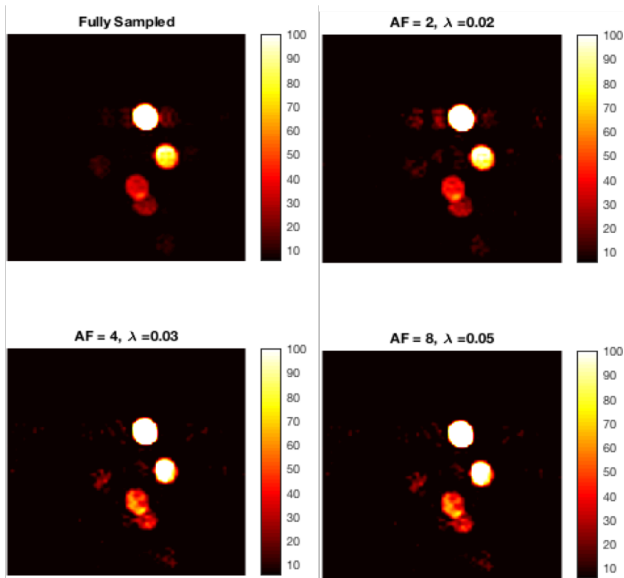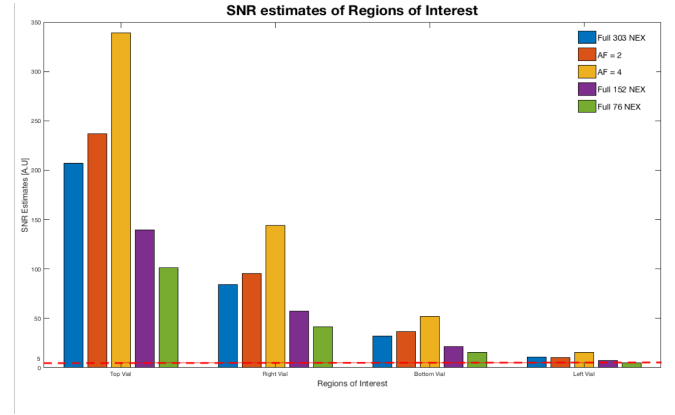
Figure 4: Optimal CS reconstructions at AF of 2, 4, and 8. Note the increased visibility of the left-most vial as AF increases. Furthermore, the increase in blurring and chemical shift artifact are more visible as AF increases. These images have been windowed to the same value.